Advanced Steel Construction – Vol. 15 No. 2 (2019) 123–128
DOI: 10.18057/IJASC.2019.15.2.1

BEHAVIOUR AND MATHEMATICAL MODEL FOR SEMI-RIGID THREADED-SLEEVE CONNECTION

Su-duo Xue [1], Si-yao Li [1], Xiong-yan Li [1, *] and Chen Yao [1, 2]

[1] *Spatial Structures Research Center, Beijing University of Technology, Beijing, China*
[2] *State Grid Beijing Electric Power Company Daxing Power Supply Company, Beijing, China*
** (Corresponding author: E-mail: xiongy2006@126.com)*

ABSTRACT

Threaded-sleeve connection (TSC) is a new type of semi-rigid connection for spatial grid structures. In this paper, bending behaviour of the TSC was analyzed and a mathematical model for prediction of moment-rotation behaviour was proposed. Firstly, experiments were conducted to investigate the bending performance and damage form of the TSC. The moment-rotation curves of the specimens were obtained as well. Then, solid finite element model was established through ANSYS. Comparing the theoretical analysis and experiments, it was observed that the numerical results agreed well with the experimental data, which indicates the feasibility of the finite element analysis method. Finally, the calculation formulas of the initial moment and the initial rotation of the TSC were obtained through MATLAB curve fitting. The shape parameter n was determined. Based on the Kishi-Chen power model, the moment-rotation model of the TSC was developed. Therefore, it will be possible to take into account semi-rigid analysis for a spatial grid structure with TSC easily and find the more actual behaviour of the structure.

ARTICLE HISTORY

Received: 15 September 2017
Revised: 23 May 2018
Accepted: 18 July 2018

KEYWORDS

Spatial grid structure;
Thread-sleeve connection;
Semi-rigid behaviour;
Mathematical model;
Finite element simulation;
Experimental test

Copyright © 2019 by The Hong Kong Institute of Steel Construction. All rights reserved.

1. Introduction

The joint of spatial grid structures is regarded to be either pinned or rigid, which simplifies the design procedure normally. However, the disadvantage of such approach is the structures just working at part of their ultimate strength, thus the components of the structure are lightly stressed [1]. And most joints of spatial grid structures actually exhibit semi-rigid deformation behaviour, which contributes substantially to overall force distribution among the members [2].

Since 1980s, interest in the effect of semi-rigid joint on the behaviour of spatial grid structures has grown significantly. It is concluded from previous publications [3, 4] that the rigidity of the joints makes considerable effects on the load-displacement of spatial grid structures. Meanwhile, it is an important factor on the capacity and failure form of the structures [5-9]. Fan *et al.* [10] proposed a new classification system for joints in spatial grid structures. And some general theoretical formulations and computational algorithms have been developed for spatial grid structures. However, these theoretical methods are proposed on some assumptions, in which the bending rigidity of the joint is defined as linear elastic springs [7, 11-13], which could not reflect the non-linear rigidity of the joint clearly. Cao *et al.* [14] and Ma *et al.* [15, 16] proposed a numerical method to simulate the property of spatial grid structure with semi-rigid joints through defining the non-linear rigidity of the joints as non-linear springs. Based on this method, the first issue of the research on spatial grid structures with semi-rigid joints is seeking for an approach to predict or obtain the non-linear rigidity of the joints.

The semi-rigidity of a joint is usually described by the moment-rotation (M-θ) curve. For spatial grid structures, the semi-rigidity of most commonly used connections has been studied. The experimental study conducted by Ueki *et al.* [17] illustrated the M-θ relationships for the semi-rigid ball joints of S14, D14 and D06. Elsheikh [18] obtained the bending stiffness of one type of flexible member-end joint system through experiments. Chenaghlou [6] found that the compressive axial force had important effects on the M-θ characteristics of the MERO joints. And he proposed a three parameter exponential model of the M-θ behaviour of the ball joints and MERO joints. López *et al.* [11] investigated the rigidity of the ORTZ joints by experimental and numerical methods. Ma *et al.* [15] investigated the M-θ characteristics of bolt-ball joints, which exhibited significant non-linearity of joint response even at an early stage of loading. Fan *et al.* [19] experimentally studied the semi-rigidity of socket joints and bolt-ball joints subjected to bending with/without axial force. Cao *et al.* [14] and Ma *et al.* [15, 16] studied the semi-rigid bolt-ball joint and its application in single-layer shells.

In order to better research the mechanical properties of the spatial grid structures with semi-rigid joints, it's necessary to propose mathematical models for the prediction of the M-θ curves of these joints. Several kinds of mathematical models for M-θ curves have been proposed for steel beam-to-column joints, i.e. linear model, polynomial model, exponential model and power model [20-22]. With such models, the connections may be simulated as spring elements with M-θ behaviour in the nonlinear analysis of semi-rigid structures [14-15, 21, 23]. However, as for spatial grid structures, only a few prediction methods for the jointing systems have been proposed. Chenaghlou *et al.* [6, 24] proposed an exponential mathematical model for ball joints utilized in spatial grid structures. However, the parameters of this model (i.e. ultimate moment capacity and initial stiffness) have to be obtained by additional experimental tests or plastic analysis, which is inconvenient for its application.

Kishi and Chen [25] collected available experimental results and set up steel joint data banks, including the test data and some predictive equations for steel beam-to-column joints. Kishi-Chen power model is one of the practical models [20, 26] as illustrated in Fig. 1 and Eq. 1.

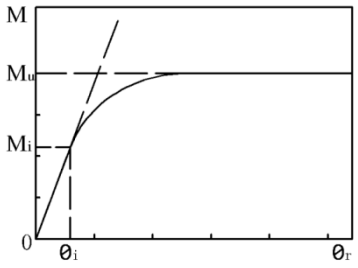

Fig. 1 Kishi-Chen power model

$$M = \frac{R_{ki}\theta_r}{\{1+(\theta_r/\theta_0)^n\}^{1/n}} \quad (1)$$

where M_i and M_u are the initial moment capacity (elastic stage) and the ultimate moment capacity respectively. M_u equals to $1.75M_i$. R_{ki} is the initial stiffness, Θ_i is the initial rotation (elastic stage), Θ_0 is the equivalent plastic rotation, $\Theta_0 = M_u / R_{ki}$, Θ_r is the arbitrary rotation and n is the shape parameter [26]. Kishi-Chen power model is still a three parameter model. In order to propose a model for joint, it's better to propose models for the initial moment, the initial rotation and the shape parameter n.

Threaded-sleeve connection for spatial grid structures, named as TSC, consists of welded ball and thread joints, and realizes the space connection of the grid structures through threads, as illustrated in Fig. 2 [27]. In order to better investigate its mechanical property, it is necessary to analyze its rigidity clearly before its application.

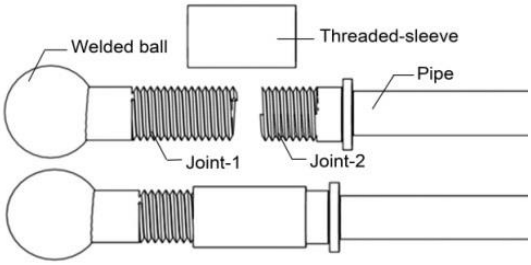

Fig. 2 Schematic of the TSC

The objective of this paper is to summarize the semi-rigid behaviour of the TSC and propose its mathematical model based on Kishi-Chen power model for prediction of *M-θ* curve. Firstly, experiments are conducted to research the bending performance and damage form of the TSC and obtain its *M-θ* curves of the specimens. Secondly, solid finite element model of the specimen is established through ANSYS and static analysis is performed to simulate the bending performance of TSC and the *M-θ* curve for comparison. Thirdly, the calculation formulas of the initial moment and the initial rotation of the TSC are derived from MATLAB curve fitting. The shape parameter n is determined. Based on the Kishi-Chen power model, the moment-rotation model of the TSC is developed.

2. Experimental study

To illustrate the bending performance and failure form of the TSC, pure bending experiments were carried out.

2.1. Specimen and instrumentation

Most geometric parameters of the TSC specimens besides the pitch of threads in this study were designed according to literature [27]. To satisfy the processing conditions, the pitch of threads for the specimens was 2 mm, which is different from 3 mm (half of the wall thickness of the joints) in literature [27]. However, it didn't have effect on semi-rigid behaviour of the TSC. Two kinds of steel with yield strength of 235MPa and 345MPa named as Q235 and Q345 were utilized for joints and tube respectively [28]. Therefore, the strength of tubes is much larger than that of the joints, which ensures that the joints yield or break earlier than structural members. The material properties of Q235 were obtained from tensile tests on coupons according to the Chinese mechanical testing standard [29]. The tested yield strength, the ultimate tensile strength and the elastic modulus of Q235 is 245.5 MPa, 383.3 MPa and 181.8 GPa, respectively.

The details of the connection are shown in Fig. 3, in which the size of the welded ball was Φ200 mm×8 mm, and the wall thickness of Joint-1 and Joint-2 was 4 mm. And the pitch of the threads was 2 mm. The greater wall thickness of the tubes is provided to prevent the instability and local buckling in the tube earlier than the failure of the joints [19]. The small square steels on the specimens were used to fix the dial gauges. The short tube on the bottom of the ball was used to test the horizontal displacement of the specimen, which enables the reduction of the measurement error of vertical displacement.

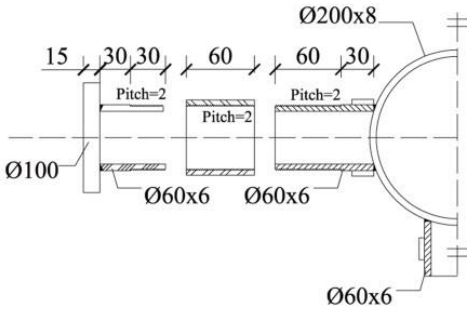

(a) The configurations of connection

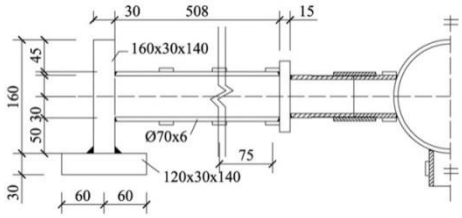

(b) The configurations of specimen

Fig. 3 The details of specimen (mm)

2.2. Loading scheme

Fig. 4(a) presents the loading frame for the experiments, which shares sufficient stiffness. The forces were loaded through two manual screw lifts and measured by force sensors. The support form was hinged by setting the specimen on the solid round steel bar, shown in Fig. 4(b). The strain gauges were located at the end of the tube, the end of the joints and middle of the threaded-sleeve, shown in Fig. 5. The gauge at the end of the tube is to monitor the tube failure in the whole load steps. The displacements were measured by dial gauges. The arrangements of the force sensors and dial gauges are also shown in Fig. 5.

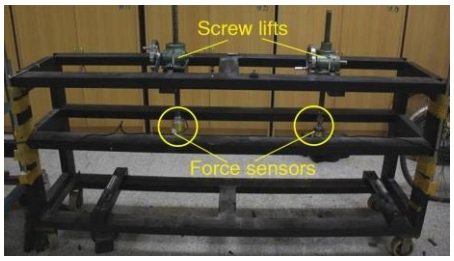

(a) Loading frame (b) Support form

Fig. 4 Loading frame and support form

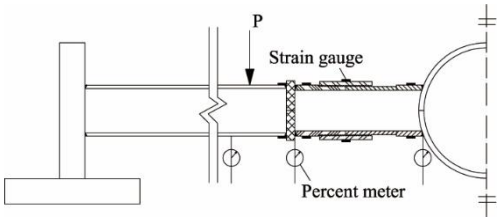

Fig. 5 The arrangement of strain gauges and force sensors

In first stage, the specimens were subjected to a small load and unloaded in order to ensure the loading apparatus and the dial gauges were working properly, which will allow the different parts of the specimen to work as a whole [19]. During the test, load increment of every step was 0.5 kN. Due to the symmetrical load of the two lifts, the whole connection was stayed in pure bending. The bending moment was applied by means of the load (*P*) and the distance between the load point and the support (*L*). Each load step kept 15 minutes to ensure the stability of the test results. The rotation could be calculated with the displacements of each part. Fig. 6 depicts the loading and bending moment calculation diagram for specimens subjected to pure bending.

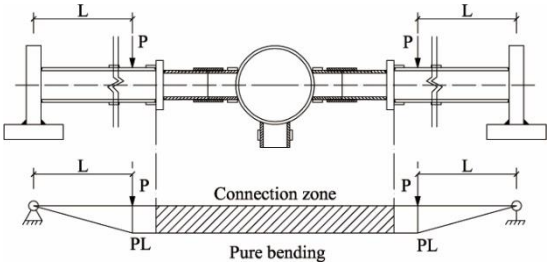

Fig. 6 Loading condition and mechanical diagram

2.3. Experimental results

The failure of the specimens can be describes as two steps. Step 1: the extended part of threads yielded and the specimen flexed, as shown in Fig. 7(a). During this step, the extended parts of the threads yielded, which indicates the connection out of work. Step 2: one thread of Joint-1 engaged with the sleeve (on the tensile area) slid out from the sleeve, as shown in Fig. 7(b). This failure process could be called thread stripping, which resulted from the deformation un-compatibility and contact status change between the threaded-sleeve, Joint-1 and Joint-2 during loading. However, after the tripping finished, the connection was able to continue bearing the load without occurrence of brittle failure, since the load could continue to redistribute to another thread. This is a positive feature of the TSC.

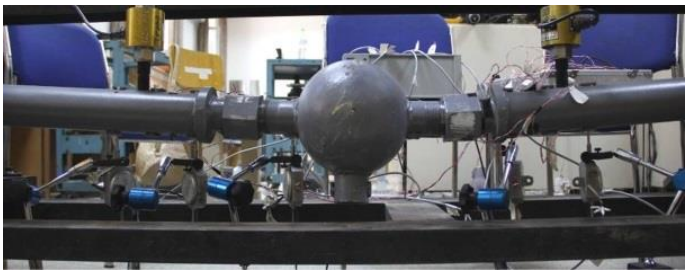

(a) Step 1: flexure

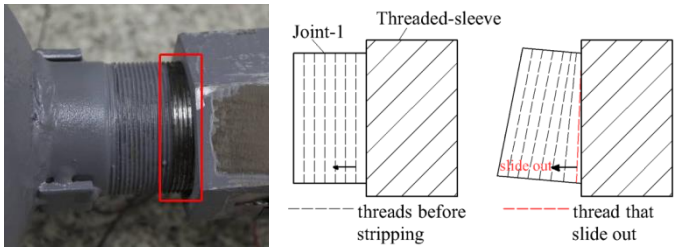

(b) Step 2: thread stripping

Fig. 7 Failure forms of the specimens

The bending performance of the connections can be represented by *M-θ* curves that describe the relationship between the applied bending moment M and the corresponding rotation θ of the connection. Fig. 8 shows the *M-θ* curves of the specimens subjected to pure bending. During the initial stage, with the increasing of the moment, the rotation of the specimens increases linearly (elastic stage). The average initial bending stiffness of specimens is around 492.6 kN·m/rad. When the moment reaches 2.6 kN·m (average value of the specimens), the growth trend slows down. The moment here refers to the moment of the interface of the Joint-2 and the tube. The average post-limit stiffness of specimens is around 126.6 kN·m/rad.

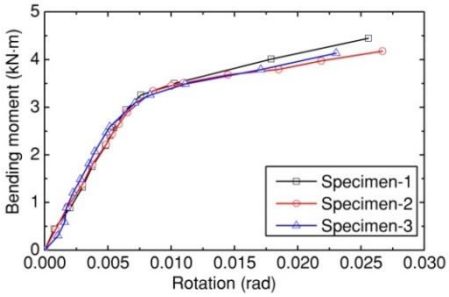

Fig. 8 *M-θ* curves of the specimens

3. Numerical simulation

3.1. FEA model

Finite element analysis (FEA) for TSC were performed with the program ANSYS. The FEA model of the specimen is established according to literature [27]. The threads were simplified as horizontal zigzags [30, 31].

The material of the TSC model is Q235, with elastic modulus *E* of 2.01×10^5 MPa and Poisson's ratio of 0.3. The measured yield strength of the material is 250 MPa. Q235 is anisotropic bilinear hardening material with strain-hardening modulus of 0.02 [32, 33].

The model is meshed with hexahedral solid elements Solid185 in ANSYS, and contact elements Targe170 and Conta174 are used to simulate the contact pairs between threads and the contact pairs between the end faces of joints, see Fig. 9(a). All the contact pairs are surface-surface contact and are set as type of Standard. Coulomb friction is used in the tangent direction of the contact surface. For contact between threads, the friction coefficient is 0.12 [34-35]. And for contact between Joint-1 and Joint-2, the friction coefficient is 0.3 [34].

All FEA models are performed with the nonlinear geometry. In order to simulate the features of the TSC, the nodes of the left hemisphere of the welded hollow ball joint are fixed, which makes the connection subjected to pure bending, see Fig. 9(b).

A Mass 21 element with small mass of 0.0001kg is established in the center of the surface 1-2 and coupled with all nodes in this surface to simulate the bending state of the connection. The bending moment is loaded on this element, as shown in Fig. 9(b).

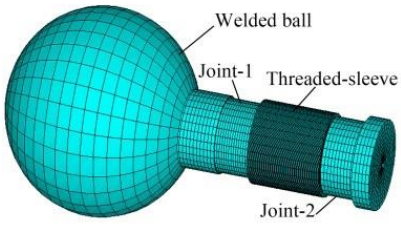

(a) Meshing of FEA model

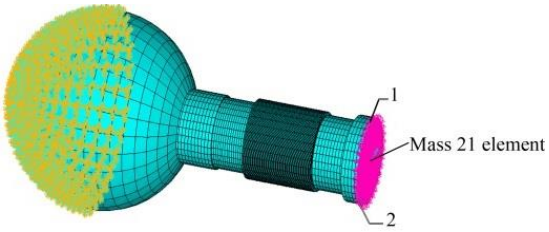

(b) Boundary conditions and load

Fig. 9 Meshing and boundary condition of FEA model

3.2. Simulation results

Fig. 10 shows the von-mises stress nephogram of the specimen under moment of 2.0 kN·m. The stress nephogram of the integral model is shown in Fig. 10(a). Due to the small geometric size, the stress concentration is easy to occur between the threads. This should be ignored in the discussion. Fig. 10(b) presents the stress nephogram of the welded ball. The maximum stress is 233 MPa. As illustrated in Fig. 10(c), the maximum stress of the joints situates at the extended part of threads. The stress of the compression zone is larger than that of the tension zone. Fig. 10(d) is the stress nephogram of the threaded-sleeve, the maximum stress situates at the middle. Overall, the most weakness area of the TSC locates in the extended part of threads of Joint-1, which agrees with the failure step 1 of the tests.

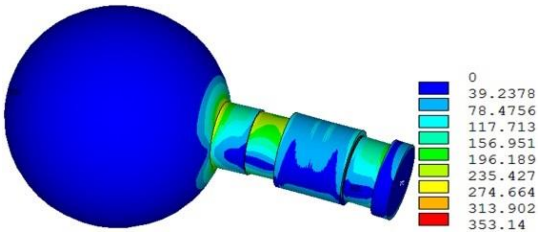

(a) The stress nephogram of the integral model

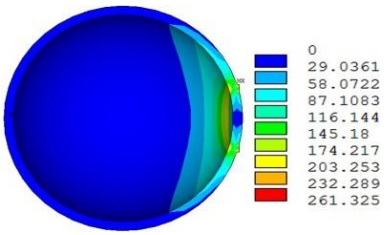

(b) The stress nephogram of welded ball

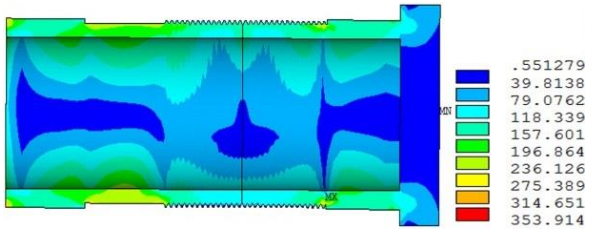

(c) The stress nephogram of joint-1 and joint-2

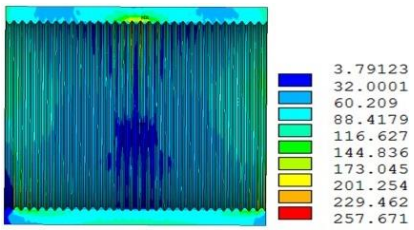

(d) The stress nephogram of the sleeve

Fig. 10 The stress nephogram of the model (MPa)

3.3. Comparison between the numerical results and experimental data

Fig. 11 presents the comparison between the *M-θ* curves of the FEA model and the specimens. The initial moment of the FEA model is 2.5 kN·m, and it is about 3.85% smaller than that of the average test results. The initial stiffness of the FEA model is 587.3 kN·m/rad, which is about 9% larger than that of the tests. The average post-limit stiffness of the FEA model is 19.1 kN·m/rad, which is about 19.2% larger than that of the tests. The error between the tests data and the simulation results possibly comes from not only the adoption of experience value for the friction coefficient of the specimens used in the simulation, but also the hard determination of the practical machining accuracy of the threads.

Fig. 12 illustrates the stress of partial measuring points (i.e. tips of Joint-1 and Joint-2, middle of the threaded sleeve) of the FEA model and Specimen-2. As illustrated in Fig. 12, it is shown that the FEA method can simulate the stress state of the specimen accurately.

The comparisons above illustrate that the numerical model provides a reasonable estimation of the practical behaviour of the TSC.

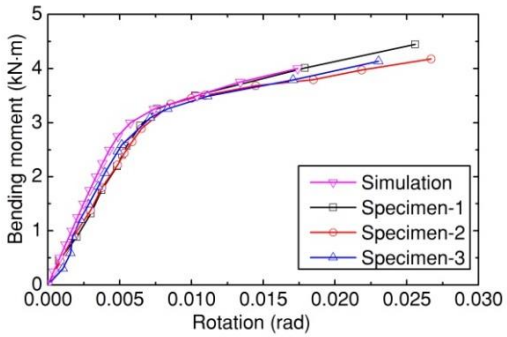

Fig. 11 Comparison of tests data and simulation results

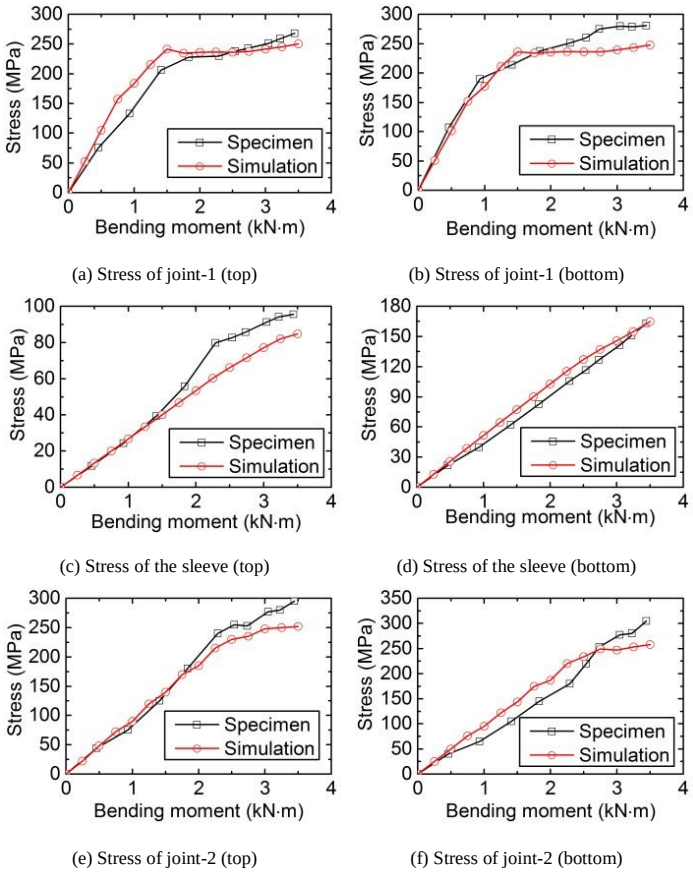

(a) Stress of joint-1 (top) (b) Stress of joint-1 (bottom)

(c) Stress of the sleeve (top) (d) Stress of the sleeve (bottom)

(e) Stress of joint-2 (top) (f) Stress of joint-2 (bottom)

Fig. 12 Comparison of stress for TSC

3.4. Parametric analysis

According with literature [27], the pitch of threads is half of the wall thickness of the joints. Thus, the influence factors on the bending performance of the TSC are the material of the connection, outer-diameter and wall thickness of the joints. On the basis of the FEA method proposed in this section, to discuss the influence of the parametric of the TSC on its bending performance, this study obtained 90 groups of *M-θ* curves of different connections with material of Q235 and Q345, outer-diameters of joints of 32 mm-160 mm, wall thickness of joints from 3 mm to16 mm.

Fig. 13 shows the influence of diameter of joints on initial moment of the connections. It is obviously that the initial moment increases with the increasing of diameters nonlinearly. Fig. 14 presents the influence of wall thickness of joints. Moreover, the initial moment increases with the increasing of wall thickness.

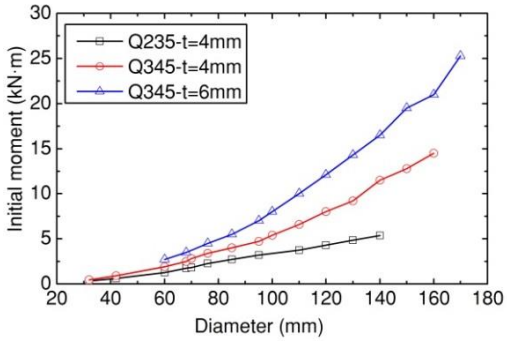

Fig. 13 Influence of diameter on initial moment

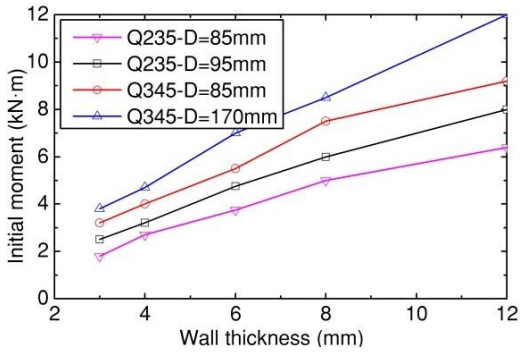

Fig. 14 Influence of wall thickness of joints on initial moment

4. Mathematical model

4.1. Mathematical model derivation

The preceding research studied the semi-rigidity of TSC, and proposed its FEA method. However, the simulation method is complex for further research and its application in real project. Thus, a mathematical model for semi-rigid behaviour of the TSC is needed. Hence, the model of TSC is proposed on the basis of Kishi-Chen power model in this paper.

The following basic assumptions are made:

(1) The material is assumed to be linearly elastic perfectly plastic for the connection;

(2) The deformation of the connection assemblage is relatively small;

(3) The failure occurs as the plastic collapse mechanism is formed in the connection.

Eq. 2 is the calculating formula for the initial bending moment of tube with circular cross section. Based on Eq. 2, the calculating formula for the initial bending moment of the TSC is obtained through MATLAB curve fitting, as illustrated in Eq. 3.

$$M_{max} = [\sigma]W_z = [\sigma]\frac{\pi}{32D}[D^4 - (D-t)^4] \tag{2}$$

$$M_i = \frac{\pi}{32D}[(0.9022D)^4 - (0.9060D - 1.9325t)^4][\sigma] \tag{3}$$

In Eq. 2 and 3, D is the outer-diameter of Joint-1 and Joint-2, t is the wall thickness of the joints and $[\sigma]$ is the allowable stress of the material.

The calculation formula for moment can be described as

$$M_{max} = \frac{\theta EI}{L} \tag{4}$$

where E is the elastic modulus, I is the inertia moment and L is the effective calculating length.

On the basis of Eqs. 3-4, the calculation method for the initial rotation of the TSC is obtained through MATLAB curve fitting, as shown in Eq. 5.

$$\theta_i = \frac{[\sigma](10.731+95.108P)}{DE} \tag{5}$$

where P is the pitch of threads, $P=t/2$.

Thus, the initial bending stiffness (R_{ki}) of the TSC is equal to M_i / Θ_i. The equivalent plastic rotation (Θ_0) is equal to M_u / R_{ki}.

Based on the Kishi-Chen power model (Eq. 1), different shape parameters (n) for TSC with different configurations were obtained through curving fitting as well, as shown in Table 1.

Table 1
Shape parameters (n) of the TSC

Outer-diameter of Joints /mm	n
32≤Φ<95	2.2
95≤Φ<130	2.1
130≤Φ≤170	2.7

Based on Eq. 3, Eq. 5 and Table 1, the mathematical model for semi-rigid behaviour of the TSC can be summarized as

$$M = \frac{M_i\theta_r}{\theta_i\{1+(0.5714\theta_r/\theta_i)^n\}^{1/n}} \tag{6}$$

4.2. Mathematical model validation

According to Eq. 3, the initial moment of the specimen is 2.1 kN·m, which is 10.5% larger than the average result of the specimens. As the pitch of the specimens is not strictly machined in accordance with literature [27], and the ratio of pitch to wall thickness has great influence on the M-θ behaviour of the connection, the M-θ curves of the specimens are not appropriate to validate the fitting effect of the proposed mathematical model here.

Take 4 connections (C1-C4) as numerical examples to validate the proposed mathematical model. The material and geometric parameters are shown in Table 2.

Table 2
Material and parameters of C1-C4

No.	Material	Outer-diameter of Joints /mm	Wall thickness of Joints /mm	Pitch of threads /mm
C1	Q235	60	4	2
C2	Q345	60	4	2
C3	Q235	140	8	4
C4	Q345	140	8	4

Fig. 15 compares the M-θ curves of C1-C4 obtained through FEA method and the proposed mathematical model. It is observed that the proposed mathematical model agrees well with the FEA method, which indicating that the mathematical model can predict well the semi-rigid behaviour of the TSC. It will be useful for the further research on the mechanical performance of single-layer spatial grid structures with TSC.

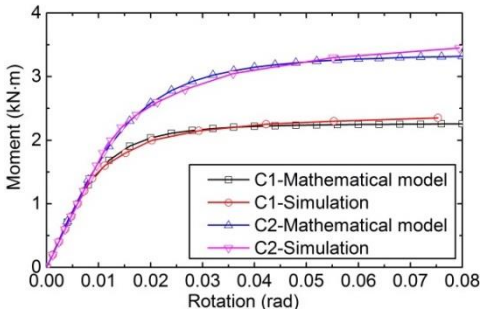

(a) M-θ curves of C1 and C2

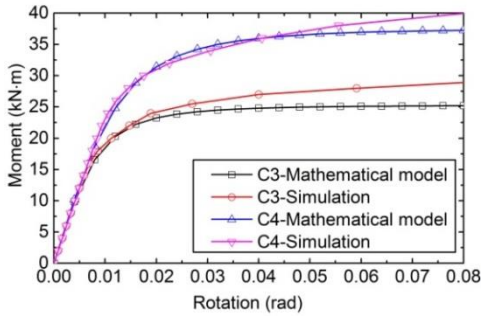

(b) M-θ curves of C3 and C4

Fig. 15 Comparison of M-θ curves based on different methods

5. Conclusions

In this paper, the semi-rigid behaviour of the TSC is studied through pure bending experiments and numerical simulation. And its mathematical model based on Kishi-Chen power model for prediction of M-θ curve is proposed. The main conclusions of the investigation are summarized as follows:

(1) Pure bending experiments are conducted to study the bending performance and damage form of the TSC and obtain the M-θ curves of the specimens. The failure process of the TSC is flexure first and then followed by thread stripping. After the stripping, the connection is able to continue bear the bending, and there is no brittle failure or broken in the tests.

(2) The FEA model of the specimen is established through ANSYS. The

bending performance of the TSC is analyzed and the *M-θ* curve is obtained to compare with the test results. It is illustrated that the numerical results fit well with the test data, indicating that the FEA method can provide a reasonable estimation of the practical behavior of TSC.

(3) On the basis of a series of parametric analysis, the calculation formula of the initial moment and the initial rotation of TSC are obtained through MATLAB curve fitting. The shape parameter n of TSCs with different outer-diameters of joints is determined.

(4) Based on Kishi-Chen power model, the *M-θ* mathematical model of the TSC is obtained. The validity of this model has been verified using four numerical examples. The model has been found to perform well for TSC. Therefore, it will be possible to take into account semi-rigid analysis for a spatial grid structure with TSC easily and find the more actual behaviour of the structure. In spatial grid structures, most joints exhibit semi-rigid behaviour. It will be useful for the design and application of spatial grid structures with semi-rigid joints.

Acknowledgments

The authors are grateful to the financial support of National Natural Science Foundation of China (Grant Nos.: 51578019 and 51378031) and the Beijing Natural Science Foundation (Grant No.:8152006).

References

[1] Turvey G.J., "Analysis of pultruded glass reinforced plastic beams with semi-rigid end connections", Composite Structures, 38(1-4), 3-16, 1997.
[2] Emmanuel A. and Glenn M., "Moment-rotation functions for steel connections", Journal of Structural Engineering, 117(6), 1703-1718, 1991.
[3] See T. and McConnel R.E., "Large displacement elastic buckling of space structures", Journal of Structural Engineering, 5(112), 1052-1069, 1986.
[4] Fathelbab F.A., The Effect of Joints on the Stability of Shallow Single Layer Lattice Domes, Ph.D. Dissertation, University of Cambridge, Cambridge, 1987.
[5] López A., Puente I. and Serna M.A., "Numerical model and experimental tests on single-layer latticed domes with semi-rigid joints", Computers and Structures, 85(7), 360-374, 2007.
[6] Chenaghlou M.R., Semi-Rigidity of Connections in Space Structures, Ph.D. Dissertation, Department of Civil Engineering, University of Surrey, Guildford, October, 1997.
[7] Chenaghlou M.R. and Nooshin H., Response of Semi-Rigidly Jointed Space Structures, Space Structures 5, Thomas Telford, 2002.
[8] Kato S., Mutoh I. and Shomura M., "Collapse of semi-rigidly jointed reticulated domes with initial geometric imperfections", Journal of Constructional Steel Research, 48(2), 145-168, 1998.
[9] Zhang H.D. and Han Q.H., "A Numerical investigation of seismic performance of large span single-layer latticed domes with semi-rigid joints", Structural Engineering and Mechanics, 48(1), 57-75, 2013.
[10] Fan F., Ma H.H., Cao Z.G. and Shen S.Z., "A new classification system for the joints used in lattice shells", Thin-Walled Structures, 49(12), 1544-1553, 2011.
[11] López A., Puente I. and Serna M.A., "Direct Evaluation of the buckling loads of semi-rigidly jointed single-layer latticed domes under symmetric loading", Engineering Structures, 29(1), 101-109, 2007.
[12] Lee K.S. and Han, S.E., "Semi-rigid elasto-plastic post buckling analysis of a space frame with finite rotation", Advanced Steel Construction, 7(3), 274-301, 2011.
[13] Shon S.D, Hwang K.J. and Lee S.J., "Numerical evaluation of buckling behaviour in space structure considering geometrical parameters with joint rigidity", J. Cent. South Univ., 21(3), 1115-1124, 2014.
[14] Cao Z.G., Du P., Chen Z.M. and Wan Z.S., "The stability and stressed skin effect analyses of an 80m diameter single-layer latticed dome with bolt-ball joints", International Journal of Steel Structures, 16(2), 279-288, 2016.
[15] Ma H.H., Fan F. and Shen S.Z., "Numerical parametric investigation of single layer latticed domes with semi-rigid joints", Journal of the International Association for Shell and Spatial Structures, 49(2), 99-110, 2008.
[16] Ma H.H, Fan F., Wen P. and Shen S.Z., "Experimental and numerical studies on a single-layer cylindrical reticulated shell with semi-rigid joints", Thin-Walled Structures, 86, 1-9, 2015.
[17] Ueki T., Matsushita F., Shibata R. and Kato S., "Design procedure for large single-layer latticed domes", Space Structures, 4(1), 237-246, 1993.
[18] Elsheikh A.I., "Numerical analysis of space trusses with flexible member-end joints", International Journal of Space Structure, 8(3), 189-197, 1993.
[19] Fan F., Ma H.H., Chen G.B. and Shen S.Z., "Experimental study of semi-rigid joint systems subjected to bending with and without axial force", Journal of Constructional Steel Research, 68(1), 126-137, 2012.
[20] Kim S.E. and Choi S.H., "Practical advanced analysis for semi-rigid space frames", International Journal of Solids & Structures, 38, 9111-9131, 2001.
[21] Liew J.Y.R., Chen W.F. and Chen H., "Advanced inelastic analysis of frame structures", Journal of Constructional Steel Research, 55(1), 245-265, 2000.
[22] Hsieh S.H., "Analysis of Three-Dimensional Steel Frames with Semi-Rigid Connections", Structural Engineering Report 90-1, School of Civil and Environmental Engineering, Cornell University, Ithaca, NY, 1990.
[23] Chen W.F., Goto Y. and Liew J.Y.R., "Stability Design of Semi-Rigid Frames", John Wiley & Sons Inc, New York, 1996.
[24] Chenaghlou M.R., Nooshin H. and Harding J.E., "Proposed mathematical model for semi-rigid joint behaviour (*M-θ*) in space structures", International Journal of Space Structures, 29(2), 71-80, 2014.
[25] Kishi N. and Chen W.F., "Semi-rigid steel beam to column connections: data base and modeling", Journal of Structural Engineering, 115(1), 105-109, 1989.
[26] Kishi N. and Chen W.F., "Moment-rotation relations of semi-rigid connections with angles", Journal of Structural Engineering, 116(7), 1813-1834, 1990.
[27] Li S.Y., Li X.Y., Xue S.D. and Ye J.H., "Strength performance of threaded-sleeve connector under axial force", Advances in Structural Engineering, 19(7), 1177-1189, 2016.
[28] GB/T 700-2006, "Carbon Structural Steels", 2006, Beijing, Standards Press of China. (in Chinese)
[29] GB/T 2975-1998, "Steel and Steel Products-Location and Preparation of Test Pieces for Mechanical Testing", 1998, Beijing, Standards Press of China. (in Chinese)
[30] Liu N. and Bu G.G., "Calculation of load capacity of bolt hole", Proceedings of the 5th China CAE Engineering Analysis Technical Conference, Lanzhou, China, 170-172, 2009. (in Chinese)
[31] Tanaka M., Miyazawa H., Asaba E. and Hongo K., "Application of the finite element method to bolt-nut joints - fundamental studies on analysis of bolt-nut joints using the finite element method", Bulletin of the JSME, 24(192), 1064-1071, 1981.
[32] Chen J., "Stability of Steel Structures Theory and Design", Science Press, Beijing, 2001. (in Chinese)
[33] Guo B. and Liu F., "Strength and stiffness of tubular L-joints", Engineering Mechanics, 22(6), 1047-1059, 2005. (in Chinese)
[34] Eugene A. A., Theodore B. III and Ali M. S., "Mark's Standard Handbook for Mechanical Engineers", 11th Edition, McGraw-Hill Companies, Inc, New York, 2007.
[35] Satoshi I., Takashi Y., Atsushi I. and Shinsuke S., "Three-dimensional finite element analysis of tightening and loosening mechanism of threaded fastener", Engineering Failure Analysis, 12(4), 604-615, 2005.